

# Clonal evolution in myeloma: the impact of maintenance lenalidomide and depth of response on the genetics and sub-clonal structure of relapsed disease in uniformly treated newly diagnosed patients

John R. Jones,<sup>1,2</sup> Niels Weinhold,<sup>3</sup> Cody Ashby,<sup>3</sup> Brian A. Walker,<sup>3</sup> Chris Wardell,<sup>3</sup> Charlotte Pawlyn,<sup>1,2</sup> Leo Rasche,<sup>3</sup> Lorenzo Melchor,<sup>2</sup> David A. Cairns,<sup>4</sup> Walter M. Gregory,<sup>4</sup> David Johnson,<sup>2</sup> Dil B. Begum,<sup>2</sup> Sidra Ellis,<sup>2</sup> Amy L. Sherborne,<sup>3</sup> Gordon Cook,<sup>5</sup> Martin F. Kaiser,<sup>1,2</sup> Mark T. Drayson,<sup>6</sup> Roger G. Owen,<sup>5</sup> Graham H. Jackson,<sup>7</sup> Faith E. Davies,<sup>3</sup> Mel Greaves<sup>2</sup> and Gareth J. Morgan;<sup>3</sup> on behalf of the NCRI Haemato-Oncology CSG

<sup>1</sup>Department of Haematology, The Royal Marsden Hospital NHS Foundation Trust, London, UK; <sup>2</sup>The Institute of Cancer Research, London, UK; <sup>3</sup>Myeloma Institute, University of Arkansas for Medical Sciences, Little Rock, AR, USA; <sup>4</sup>Clinical Trials Research Unit, Leeds Institute of Clinical Trials Research, University of Leeds, UK; <sup>5</sup>Leeds Institute of Cancer and Pathology, University of Leeds, UK; <sup>6</sup>Clinical Immunology, School of Immunity and Infection, University of Birmingham, UK and <sup>7</sup>Northern Institute for Cancer Research, Newcastle University, Newcastle upon Tyne, UK

©2019 Ferrata Storti Foundation. This is an open-access paper. doi:10.3324/haematol.2018.202200

Received: August 31, 2018.

Accepted: January 30, 2019.

Pre-published: February 7, 2019.

Correspondence: GARETH J. MORGAN - [gjmorgan@uams.edu](mailto:gjmorgan@uams.edu)

---

Supplementary Table 1. Characteristics according to induction treatment

	Induction	
	Lenalidomide (% of group)	Thalidomide (% of group)
<b>Patient numbers</b>	27 (52)	29 (48)
<b>Best response</b>		
CR series (CR/nCR)	12 (44)	12 (41)
Non-CR series (VGPR/PR)	15 (56)	17 (59)
<b>Median PFS (months, range)</b>	19 (8-51)	19 (8-34)
<b>Presentation ISS</b>		
I	6 (22)	7 (24)
II	11 (41)	10 (34)
III	10 (37)	11 (38)
Missing		1 (3)
<b>Evolutionary mechanism</b>		
Branching	20 (74)	17 (59)
Linear	3 (11)	8 (28)
Stable	4 (15)	4 (14)
<b>Non-synonymous mutational load</b>		
Presentation	37	40
Relapse	41	58
<b>All coding mutations</b>		
Presentation	70	81
Relapse	86	102

**Supplementary Table 2. The profile of mutations known to be important in myeloma at presentation and relapse according to induction therapy.** Mutations in *KRAS*, *NRAS*, *DIS3*, *FAM46C*, *TET2*, *TRAF3* and *TP53* were seen in >5% of patients at either time point in both series. Mutations were gained and lost at relapse in both the lenalidomide and thalidomide series.

Lenalidomide induction		
Gene	Presentation	Relapse
<b>KRAS</b>	<b>26 (7)</b>	<b>30 (8)</b>
<b>NRAS</b>	<b>30 (8)</b>	<b>22 (6)</b>
<b>DIS3</b>	<b>22 (6)</b>	<b>19 (5)</b>
<i>RB1</i>	15 (4)	15 (4)
<i>ATM</i>	7 (2)	7 (2)
<b>FAM46C</b>	<b>7 (2)</b>	<b>7 (2)</b>
<b>TET2</b>	<b>7 (2)</b>	<b>7 (2)</b>
<b>TRAF3</b>	<b>7 (2)</b>	<b>7 (2)</b>
<i>EGFR</i>	4 (1)	7 (2)
<b>TP53</b>	<b>4 (1)</b>	<b>7 (2)</b>
<i>DDB1</i>	4 (1)	7 (2)
<i>BRAF</i>	7 (2)	4 (1)
<i>NF1</i>	4 (1)	4 (1)
<i>LTB</i>	4 (1)	4 (1)
<i>ATR</i>	4 (1)	4 (1)
<i>HIST1H1E</i>	4 (1)	4 (1)
<i>SETD2</i>	4 (1)	4 (1)
<i>SLC16A1</i>	4 (1)	4 (1)
<i>EGR1</i>	4 (1)	4 (1)
<i>FGFR3</i>	4 (1)	4 (1)
<i>IRF4</i>	4 (1)	4 (1)
<i>PRDM1</i>	0	4 (1)
<i>CHD2</i>	4 (1)	0
<i>FANCA</i>	4 (1)	0
<i>CRBN</i>	0	0
<i>FAF1</i>	0	0
<i>MYC</i>	0	0

Thalidomide induction		
Gene	Presentation	Relapse
<b>NRAS</b>	<b>21 (6)</b>	<b>24 (7)</b>
<b>KRAS</b>	<b>17 (5)</b>	<b>17 (5)</b>
<b>TP53</b>	<b>10 (3)</b>	<b>14 (4)</b>
<b>TRAF3</b>	<b>10 (3)</b>	<b>10 (3)</b>
<b>DIS3</b>	<b>7 (2)</b>	<b>7 (2)</b>
<i>NF1</i>	3 (1)	7 (2)
<b>TET2</b>	<b>3 (1)</b>	<b>7 (2)</b>
<b>FAM46C</b>	<b>7 (2)</b>	<b>3 (1)</b>
<i>PRDM1</i>	0	7 (2)
<i>ATM</i>	3 (1)	3 (1)
<i>ATR</i>	3 (1)	3 (1)
<i>HIST1H1E</i>	3 (1)	3 (1)
<i>CHD2</i>	3 (1)	3 (1)
<i>RB1</i>	3 (1)	3 (1)
<i>EGR1</i>	3 (1)	3 (1)
<i>FGFR3</i>	3 (1)	3 (1)
<i>IRF4</i>	3 (1)	3 (1)
<i>CRBN</i>	0	3 (1)
<i>MYC</i>	0	3 (1)
<i>FAF1</i>	0	3 (1)
<i>FANCA</i>	3 (1)	0
<i>SETD2</i>	0	0
<i>DDB1</i>	0	0
<i>SLC16A1</i>	0	0
<i>BRAF</i>	0	0
<i>EGFR</i>	0	0
<i>LTB</i>	0	0

Mutations in bold indicates they were seen in >5% of patients at either presentation or relapse in both series.

**Supplementary Table 3. MYC translocations at presentation and relapse**

Patient	MYC time point	IGH translocation	1st Chr.	1st gene	2nd Chr.	2nd gene	Induction	Maintenance	Best response
<b>Presentation and relapse</b>									
7*	Presentation and relapse	14;16 P+R	16	WWOX	8	LOC727677-MYC	CTD	Lenalidomide	VGPR
7*	Presentation and relapse	14;16 P+R	14	BRF1	8	PVT1-LOC728724			
11	Presentation and relapse	Nil	14	C14orf80-TMEM121	8	POU5F1B-LOC727677	RCD	Lenalidomide	VGPR
12*	Presentation and relapse	Nil	15	BCL2A1-ZFAND6	8	PVT1	CTDa	Lenalidomide	PR
12*	Presentation and relapse	Nil	21	PRDM15	8	PVT1-LOC728724			
29	Presentation and relapse	Nil	5	ZNF131	8	LOC727677	RCDa	Lenalidomide	VGPR
34*	Presentation and relapse	10;14 P only	9	SYK	8	LOC727677-MYC	CTD	Observation	VGPR
34*	Presentation and relapse	10;14 P only	2	EIF2AK-RPIA	8	MYC-PVT1			
36	Presentation and relapse	14;19 P only	22	TTC28	8	PCAT1-POU5F1B	RCD	Observation	PR
38	Presentation and relapse	Nil	22	TTC28	8	PCAT1-POU5F1B	RCDa	Observation	nCR
42*	Presentation and relapse	Nil	1	FAM46C	8	PVT1	CTDa	Observation	PR
42*	Presentation and relapse	Nil	1	FAM46C	8	PVT1			
46	Presentation and relapse	Nil	4	TMEM155	8	PVT1-LOC728725	CTD	Observation	PR
55	Presentation and relapse	Nil	6	DUSP22	8	PVT1-LOC728725	CTD	Observation	VGPR
56	Presentation and relapse	11;14 P+R	14	ELK2AP-KIAA0125	8	LOC727677-MYC	CTD	Observation	VGPR
<b>Relapse only</b>									
18*	Relapse only	14;16 P+R	2	LAPTM4A-SDC1	8	PVT1-LOC728724	CTDa	Lenalidomide	CR
18*	Relapse only	14;16 P+R	22	IGLL5-RTDR1	8	PVT1-LOC728724			
31	Relapse only	Nil	22	IGLL5-RTDR1	8	PVT1-LOC728724	RCDa	Observation	CR
47	Relapse only	11;14 P+R	7	COBL-POM121K12	8	PVT1	CTDa	Observation	VGPR
<b>Loss and gain</b>									
53*	Presentation only	Nil	22	IGLL5-RTDR1	8	PVT1-LOC728725	CTDa	Observation	nCR
53*	Relapse only	Nil	3	SPTA16-NLGN1	8	PCAT1-POU5F1B			

**Supplementary Table 4. Mutational load according to depth of response and maintenance allocation**

Treatment/time point		Median number of mutations	Interquartile range	p value
<b>CR series - all mutations and non-synonymous mutations only</b>				
Lenalidomide all n=14	Presentation	82	59 - 271	0.046
	Relapse	117	80 - 288	
Lenalidomide NS n=14	Presentation	42	25 - 110	0.01
	Relapse	58	41 - 124	
Observation all n=10	Presentation	65	53 - 95	0.07
	Relapse	93	64 - 152	
Observation NS n=10	Presentation	38	30 - 52	0.09
	Relapse	59	32 - 78	
Whole series all n=24	Presentation	76	58 - 115	0.008
	Relapse	102	71 - 177	
Whole series NS n=24	Presentation	40	29 - 52	<0.001
	Relapse	59	40 - 81	
<b>Non-CR series</b>				
Lenalidomide all n=16	Presentation	64	54 - 86	0.68
	Relapse	67	44 - 87	
Lenalidomide NS n=16	Presentation	37	26 - 46	0.75
	Relapse	37	22 - 44	
Observation all n=16	Presentation	85	69 - 107	0.59
	Relapse	97	69 - 140	
Observation NS n=16	Presentation	45	34 - 54	0.56
	Relapse	51	33 - 77	
Whole series n=32	Presentation	71	60 - 105	0.53
	Relapse	82	60 - 117	
Whole series n=32	Presentation	39	32 - 54	0.56
	Relapse	39	33 - 62	

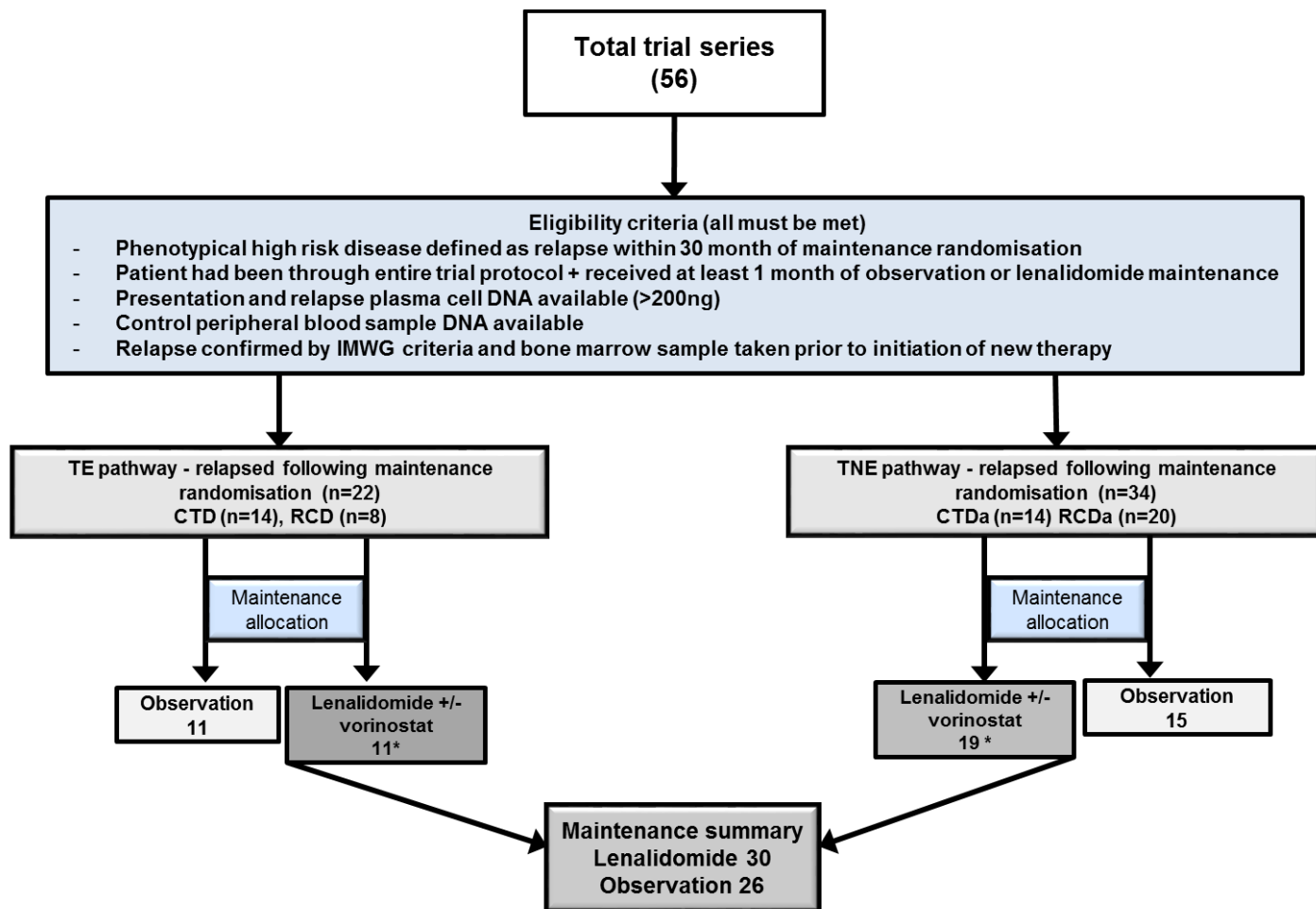
NS = Non-synonymous  
All = all coding mutations

**Supplementary Table 5. Mutational clusters at presentation and relapse**

Patient	Maintenance	Cluster change at relapse	Clusters presentation	Clusters relapse
1	Lenalidomide	Gain	7	8
2	Lenalidomide	Neutral	4	4
3	Lenalidomide	Gain	8	10
4	Lenalidomide	Gain	8	9
5	Lenalidomide	Neutral	4	4
6	Lenalidomide	Neutral	7	7
7	Lenalidomide	Neutral	6	6
8	Lenalidomide	Neutral	8	8
9	Lenalidomide	Neutral	7	7
10	Lenalidomide	Neutral	10	10
11	Lenalidomide	Loss	7	6
12	Lenalidomide	Neutral	7	7
13	Lenalidomide	Loss	8	7
14	Lenalidomide	Loss	5	4
15	Lenalidomide	Neutral	5	5
16	Lenalidomide	Neutral	2	2
17	Lenalidomide	Neutral	3	3
18	Lenalidomide	Neutral	9	9
19	Lenalidomide	Neutral	4	4
20	Lenalidomide	Gain	6	6
21	Lenalidomide	Neutral	9	9
22	Lenalidomide	Loss	3	2
23	Lenalidomide	Gain	6	7
24	Lenalidomide	Gain	5	6
25	Lenalidomide	Neutral	7	7
26	Lenalidomide	Neutral	6	6
27	Lenalidomide	Neutral	6	6
28	Lenalidomide	Gain	7	8
29	Lenalidomide	Neutral	4	4
30	Lenalidomide	Neutral	7	7
31	Observation	Neutral	4	4
32	Observation	Loss	10	9
33	Observation	Neutral	5	5
34	Observation	Gain	8	9
35	Observation	Gain	7	8
36	Observation	Loss	8	7
37	Observation	Neutral	8	8
38	Observation	Gain	6	7
39	Observation	Neutral	6	6
40	Observation	Loss	4	5
41	Observation	Loss	6	5
42	Observation	Neutral	6	6
43	Observation	Neutral	7	7
44	Observation	Gain	4	5
45	Observation	Gain	3	4
46	Observation	Neutral	5	5
47	Observation	Neutral	10	10
48	Observation	Neutral	4	4
49	Observation	Gain	6	7
50	Observation	Loss	5	3
51	Observation	Loss	8	7
52	Observation	Gain	3	4
53	Observation	Neutral	9	9
54	Observation	Neutral	6	6
55	Observation	Neutral	7	7
56	Observation	Gain	7	8

**Supplementary Table 6 – Impact of evolution on outcome according to maintenance allocation**

<b>Treatment group</b>	<b>Time point</b>	<b>PFS</b>	<b>p value</b>	<b>OS</b>	<b>p value</b>
Lenalidomide	Branching	19	0.69	36	0.58
	Non-branching	18		36	
Observation	Branching	22	0.18	46	0.73
	Non-branching	16		44	
All patients	Branching	19	0.24	37	0.13
	Non-branching	16		41	

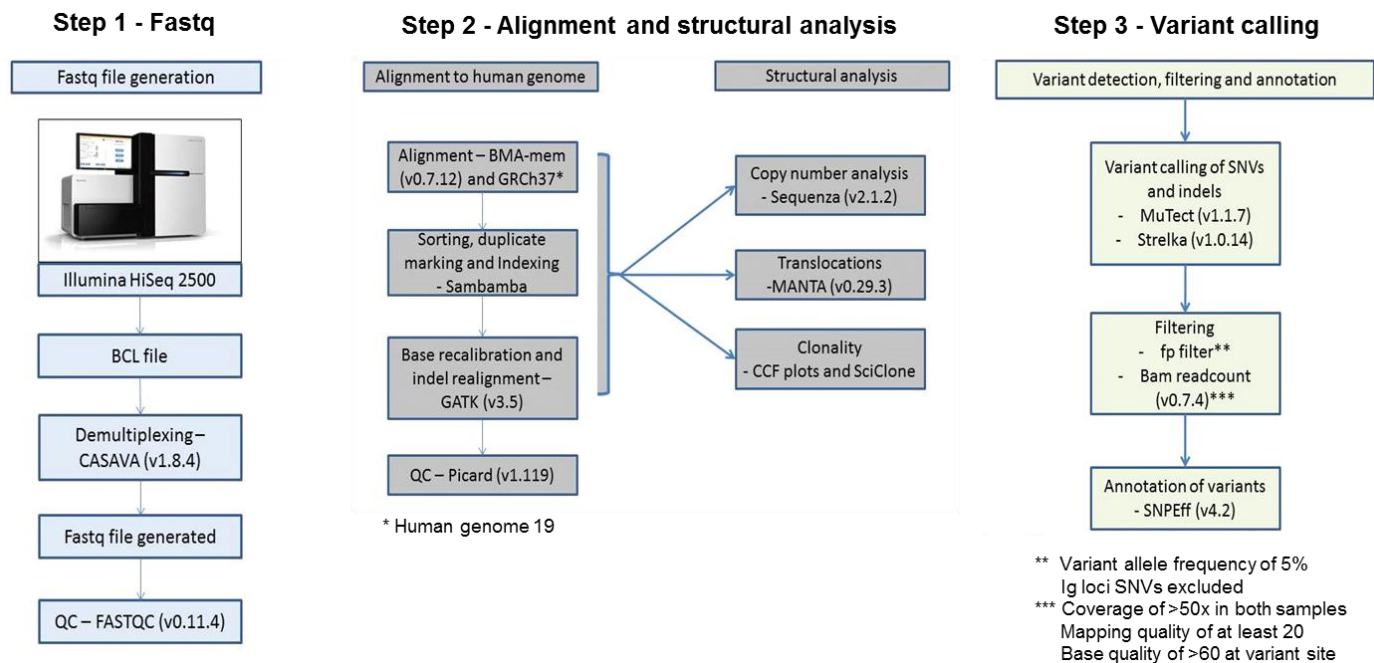


\* 3 TE and TNE patients received lenalidomide and vorinostat

**Supplementary Figure 1. Pathway for all patients included in the nested case control analysis.**

Abbreviations; TE, transplant eligible; TNE, transplant non-eligible; CTD, cyclophosphamide, thalidomide and dexamethasone; RCD, lenalidomide, cyclophosphamide and dexamethasone; a, attenuated.





**Supplementary Figure 2. Analysis pipeline.** Following preparation and indexing all samples were run on the Illumina HiSeq 2500. Conversion of BCL files to compressed Fastq files required de-multiplexing (for pooled samples) which was conducted using the package CASAVA v1.8.4 (Illumina). The package FASTQC (version 0.11, Babraham Bioinformatics) was used for basic quality checking of all Fastq files. All files were aligned to the reference human genome (GRCh37) using Burrow-Wheeler Aligner (BWA-mem version 0.7.12 (Broad institute)). This consists of a package of three algorithms that enable mapping of reads from between 70 bp – 1Mbp (1, 2). Additional indexing steps were conducted using Sambamba (version 0.5.6, GitHub), to index and mark duplicates and the Genome Analysis Toolkit (version 3.5, GATK) for base recalibration and indel realignment (3). Determination of coverage, number of duplicates and on-target percentage was performed using Picard (version 1.119, Broad institute).

Translocations involving the IgH and MYC locus were determined in all patients using the bioinformatics package Manta (version 0.29.3) (4). For 51/112 (46%) patient samples, for which enough DNA was available, translocations involving the IgH were also assessed using multiplexed real-time quantitative reverse transcriptase-PCR (qRT-PCR) and a fluorescence in-situ hybridisation-validated translocation analysis using a cyclin-D classification-based hierarchical algorithm was applied to determine the IgH translocation status (5). This formed an internal quality control and a consensus between MANTA and qRT-PCR was observed in 43/51 samples (84%). For the 8 patients where a mismatch was observed the Integrative Genomics Viewer (IGV) (version 2.3.90) was used to confirm whether a translocation was present or not (6). IGV was used to confirm all suspected MYC translocations.

CNAs for all samples were determined using the bioinformatics assessment tool Sequenza (version 2.1.2, CRAN) and where there was enough DNA multiplexed ligation-dependent probe amplification (MLPA) (SALSA MLPA P425-B1 multiple myeloma probemix, MRC Holland) was also undertaken (7, 8). Paired MLPA and Sequenza data was available for 90/112 (80%) tumour samples. A consensus between MLPA and Sequenza was observed in 85/90 samples (94%). For the five patients where a mismatch was observed Sequenza was used to determine the final profile.

Single nucleotide variants and indels were identified using MuTect (version 1.1.17, broad) and Strelka (version 1.0.14, GitHub) using the default settings (9, 10). Filtering of MuTect output was undertaken with fpfilter (github.com) with a set variant allele frequency (VAF = reference allele/variant allele corrected for copy number) threshold of 5%. Indels were called using Strelka only (VAF filter 5%). A VAF filter was required to ensure mutations were not called inappropriately, as a consequence of low level cross contamination or sequencing errors. Single nucleotide variants located with the immunoglobulin loci were excluded due to expectant non-significant variation. The R package Rsamtools (version 1.24.0, Bioconductor) for aligned sequences was used to determine read counts for each mutation. The set inclusion criteria for mutation calling included; the presence of unique reads, a mapping quality of a minimum of 20 reads and the same for base quality at variant sites and a minimum coverage of 50x for presentation, relapse and control samples for the patient. Non-silent mutations were defined as missense, frameshift, non-sense, and splice site.

For all mutations the CCF was calculated according to Stephens *et al* (2012) (11). To determine the CCF the copy number at the mutation site, tumour purity and VAF was required and the following equation applied;

$$n_{mut} = f_s * \frac{1}{p} [pn_{locus}^t + 2(1 - p)]$$

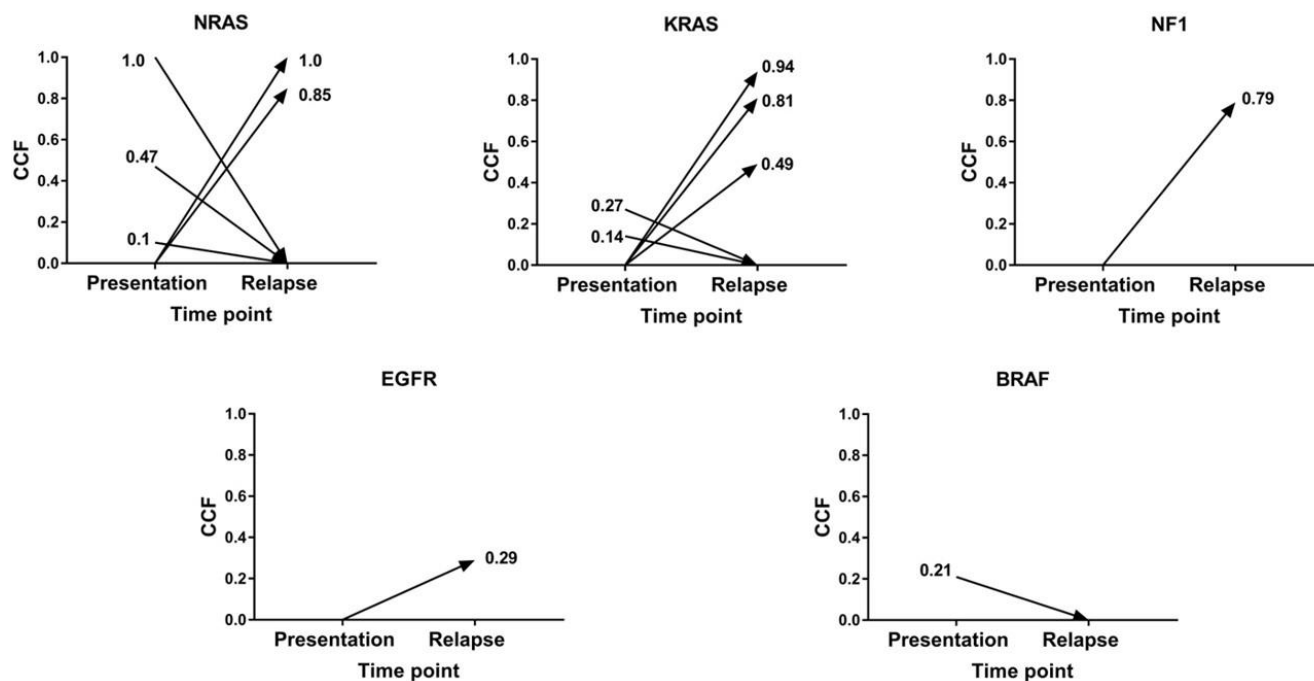
Where;  $n_{mut}$  = mutation copy number,  $f_s$  = VAF,  $p$  = tumour purity,  $n_{locus}^t$  = mutation site copy number

Purity and mutation site copy number were determined using Sequenza, with purity manually checked against the mutant allele frequency on Chromosome 14. The expected VAF was compared to values assuming the mutation was on 1, 2, ..., C chromosomes and assigned  $n_{chr}$  the value of C with binomial distribution used to determine the maximum likelihood. The CCF was then calculated by dividing  $n_{mut}$  by  $n_{chr}$ .

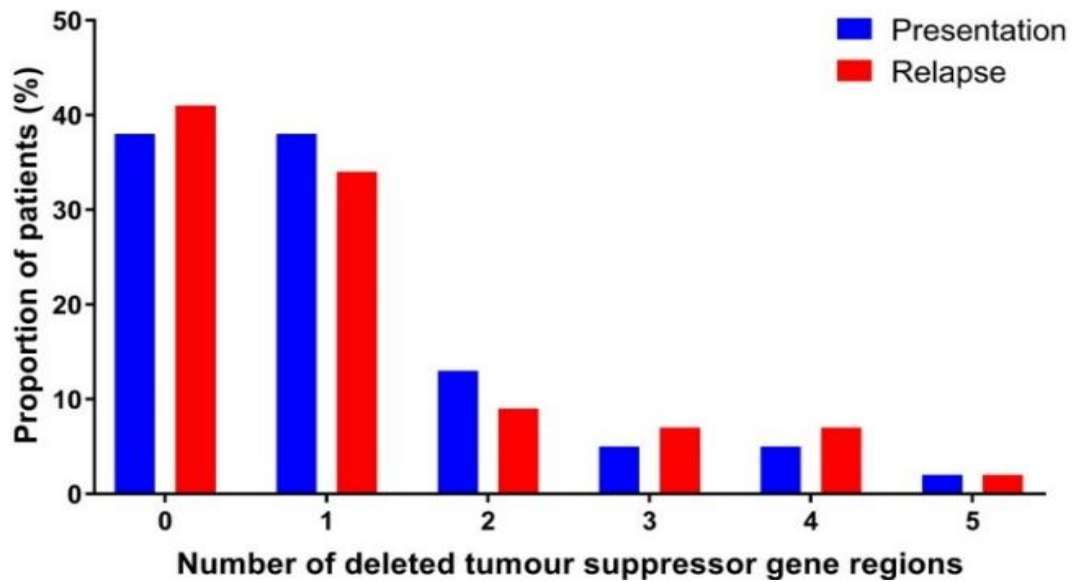
SciClone clustering, using the VAF for all coding mutations (R package version 1.1.0, GitHub) was performed to infer clusters of mutations in all patients at presentation and relapse (12). In addition, kernel density estimation plots for determining clusters of mutations according to CCF was used (R package).

#### References:

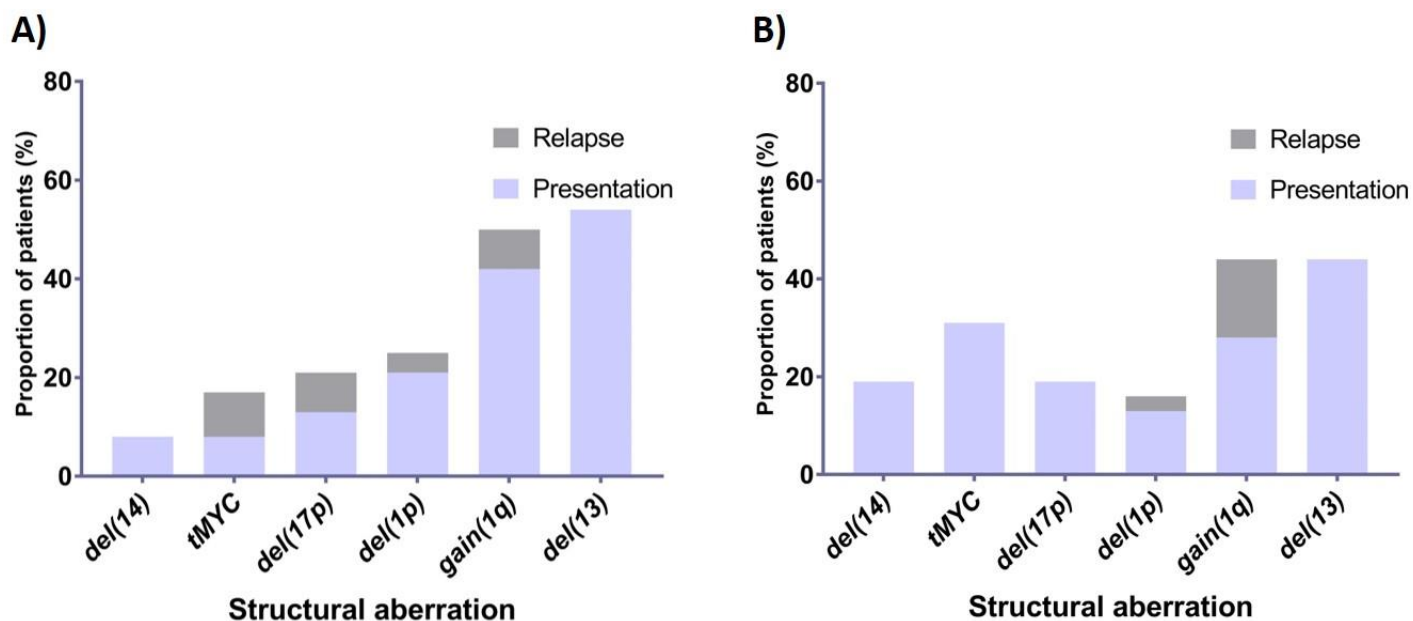
1. Li H, Durbin R. Fast and accurate short read alignment with Burrows-Wheeler transform. *Bioinformatics*. 2009;25(14):1754-60.
2. Li H, Durbin R. Fast and accurate long-read alignment with Burrows-Wheeler transform. *Bioinformatics*. 2010;26(5):589-95.
3. Tarasov A, Vilella AJ, Cuppen E, Nijman IJ, Prins P. Sambamba: fast processing of NGS alignment formats. *Bioinformatics*. 2015;31(12):2032-4.
4. Chen X, Schulz-Trieglaff O, Shaw R, Barnes B, Schlesinger F, Kallberg M, et al. Manta: rapid detection of structural variants and indels for germline and cancer sequencing applications. *Bioinformatics*. 2016;32(8):1220-2.
5. Kaiser MF, Walker BA, Hockley SL, Begum DB, Wardell CP, Gonzalez D, et al. A TC classification-based predictor for multiple myeloma using multiplexed real-time quantitative PCR. *Leukemia*. 2013;27(8):1754-7.
6. Robinson JT, Thorvaldsdottir H, Winckler W, Guttman M, Lander ES, Getz G, et al. Integrative genomics viewer. *Nat Biotechnol*. 2011;29(1):24-6.
7. Boyle EM, Proszek PZ, Kaiser MF, Begum D, Dahir N, Savola S, et al. A molecular diagnostic approach able to detect the recurrent genetic prognostic factors typical of presenting myeloma. *Genes Chromosomes Cancer*. 2015;54(2):91-8.
8. Favero F, Joshi T, Marquard AM, Birkbak NJ, Krzystanek M, Li Q, et al. Sequenza: allele-specific copy number and mutation profiles from tumor sequencing data. *Ann Oncol*. 2015;26(1):64-70.
9. Cibulskis K, Lawrence MS, Carter SL, Sivachenko A, Jaffe D, Sougnez C, et al. Sensitive detection of somatic point mutations in impure and heterogeneous cancer samples. *Nat Biotechnol*. 2013;31(3):213-9.
10. Saunders CT, Wong WS, Swamy S, Becq J, Murray LJ, Cheetham RK, Strelka: accurate somatic small-variant calling from sequenced tumor-normal sample pairs. *Bioinformatics*. 2012;28(14):1811-7.
11. Stephens PJ, Tarpey PS, Davies H, Van Loo P, Greenman C, Wedge DC, et al. The landscape of cancer genes and mutational processes in breast cancer. *Nature*. 2012;486(7403):400-4.
12. Miller CA, White BS, Dees ND, Griffith M, Welch JS, Griffith OL, et al. SciClone: inferring clonal architecture and tracking the spatial and temporal patterns of tumor evolution. *PLoS Comput Biol*. 2014;10(8):e1003665.



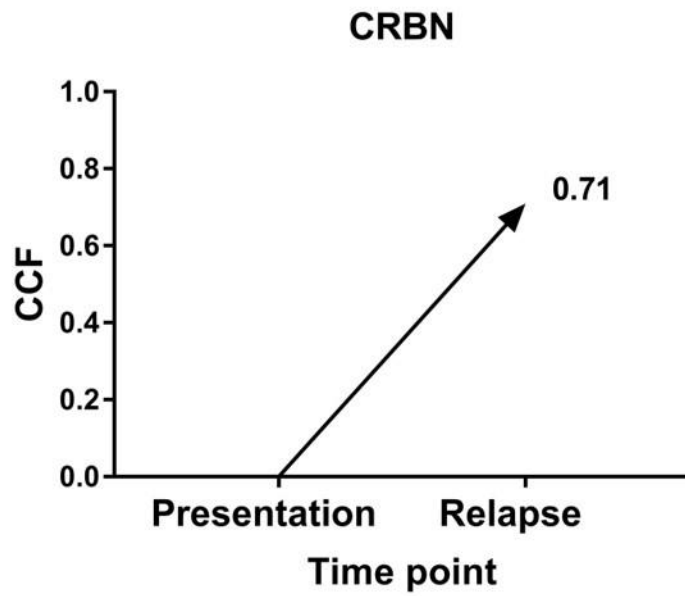
**Supplementary Figure 3. Cancer clonal fractions of RAS pathway mutations gained and lost at relapse.** New mutations of the MAPK pathway genes, *NRAS*, *KRAS*, *NF1* and *EGFR* were seen in 13% (7/56) patients at relapse. Importantly most of these new mutations were clonal at relapse, with CCF values of greater than 80%, suggesting a marked change in clonal dominance. Mutations in *NRAS*, *KRAS* and *BRAF* were also lost in 9% (5/56) patients at relapse.



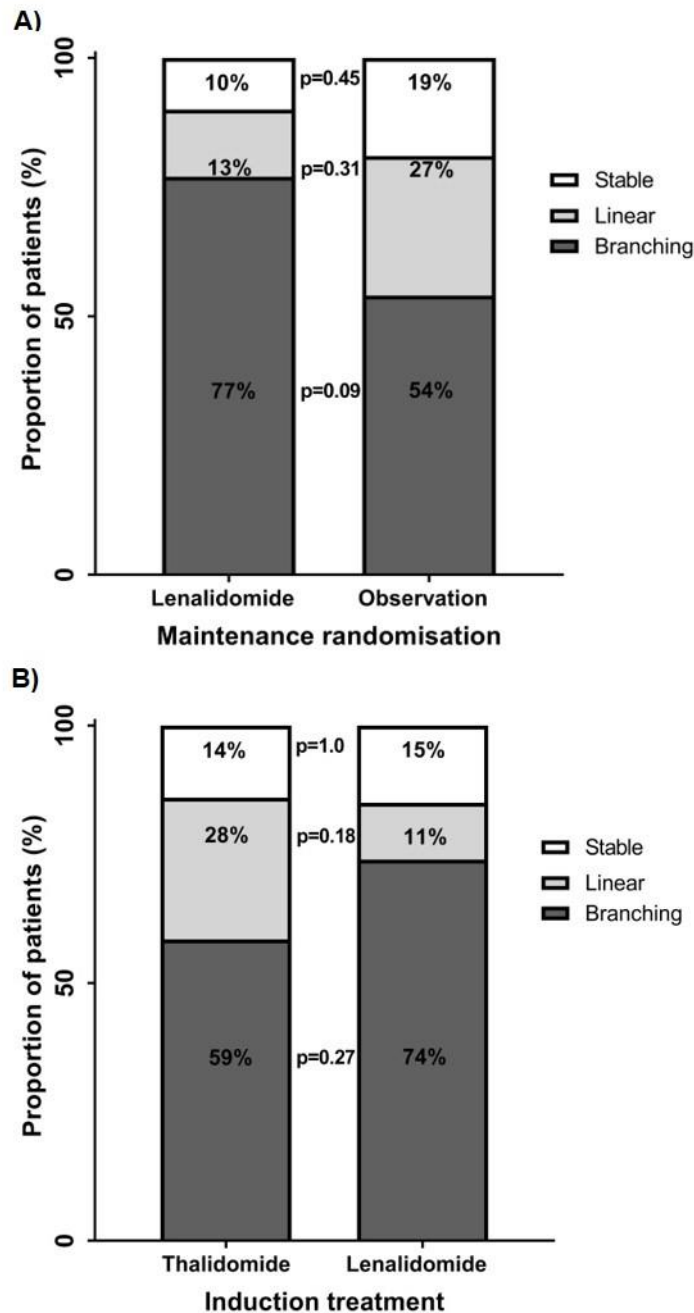
**Supplementary Figure 4. Structural aberration profile at presentation and relapse.** The number of patients with one or more prognostic tumour suppressor gene deletion remained stable at both time points, with 63% (35/56) of patients having a deletion or one or more region at presentation compared to 59% (33/56) at relapse. There was a slightly higher proportion of patients with three or more deleted regions at relapse, 16% versus 13% at presentation.



**Supplementary Figure 5. Proportion of patients with structural change at presentation and relapse. A) CR series.** A change in the profile of structural aberrations was seen in 42% (10/24) of the CR patients at relapse when compared to presentation. The gain of lesions predominated, particularly tMYC, del(17p), del(1p) and gain(1q), all of which were seen in a greater proportion of patients at relapse. **B) Non-CR series.** Only 28% of non-CR patients had a change in the structural aberration profile at relapse, with only gain(1q) and del(1p) seen in a greater proportion of patients when compared to presentation.



**Supplementary Figure 6. *CRBN* mutation cancer clonal fraction at presentation and relapse.** At presentation no *CRBN* was evident but at relapse a new mutation was found with a CCF of 0.71 suggesting it was present within a dominant clone at relapse.



**Supplementary Figure 7. Evolutionary mechanism leading to relapse according to induction and maintenance randomisation. A) Evolution according to maintenance.** Branching evolution was the predominant mechanism leading to relapse, seen in 54% of observation patients and 77% of lenalidomide maintenance patients ( $p=0.09$ , Fisher's Exact). There was also no statistical difference between the proportions of patients relapsing via linear and stable mechanisms. **B) Evolution according to induction.** Branching evolution was the predominant mechanism leading to relapse, seen in 59% of thalidomide treated patients and 74% of lenalidomide treated patients ( $p=0.27$ ). Although there was a slightly higher proportion of thalidomide patients displaying linear evolution, 28% vs 11%, this was not significant ( $p=0.18$ ). Stable progression was seen in 14% and 15% of thalidomide and lenalidomide patients respective ( $p=1.0$ ).